

Absorption-Model Analysis of $KN \rightarrow K^*(890)N$ Reactions*

JOHN T. DONOHUE†

Department of Physics, University of Illinois, Urbana, Illinois

(Received 8 June 1967; revised manuscript received 28 July 1967)

The absorptive peripheral model using a mixture of pion and vector-meson exchange is used to analyze data on $K^\pm p \rightarrow K^{*\pm}(890)p$ at momenta $\simeq 3$ GeV/c. The vector-meson exchange couplings are obtained phenomenologically by fitting the experimental data. Good fits are obtained; in particular, evidence is found for an interference effect between pion and vector-meson exchange which causes differences between K^{*+} and K^{*-} reactions. The production of neutral K^* is discussed, and an attempt is made to separate the $I=0$ and $I=1$ vector-meson exchanges. Some predictions of the model for higher energies are presented, which suggest that the known energy-dependence difficulties of vector-meson exchange will make our method inapplicable. Evidence for the interference effect in other reactions is suggested, and experimental tests are proposed.

I. INTRODUCTION

THE production and decay angular distributions in the reactions $K^\pm p \rightarrow K^{*\pm}(890)p$ have been studied in several experiments in the range 2- to 5-GeV/c incident K momenta.¹⁻⁷ The K^* decay distributions show a strong $\cos^2\varphi$ dependence in the Treiman-Yang angle, while the production differential cross section is less sharply forward peaked than that for the reaction $\pi p \rightarrow \rho p$. These properties suggest vector-meson exchange as a production mechanism, with ω , ρ , and φ allowed. Pion exchange with the known $K^*K\pi$ and $NN\pi$ couplings also occurs. With the development of the absorptive peripheral model and its success in calculating the differential cross sections and the density matrix elements for the reaction $\pi p \rightarrow \rho p$, it was hoped that the K^*p reaction might be similarly explained.^{8,9} However, the incorrect energy dependence of spin-1 exchange cross sections, even with absorption,

and the lack of knowledge of the K^*KV couplings prevent a direct comparison between theory and experiment. Instead we attempt to determine the effective vector couplings by fitting the experimental results. Couplings obtained in this way will be energy-dependent, but they may provide useful information on vector-meson exchange.

In JDGKS an attempt to obtain vector-meson couplings using the $K^{*\pm}$ experimental results at 3 GeV/c was reported. The vector and tensor couplings for the exchange of the vector-meson corresponding to ρ and ω were expressed in terms of two parameters (ξ, η) , and a search was made for values giving a good fit to the K^{*+} production data. Two regions in the (ξ, η) plane, I, with $\xi > 0$, and II, with $\xi < 0$, were found for which the fits to the experimental data were of comparable quality. Later a study of the $K^{*-}p$ reaction at 2.64 GeV/c was made, using the detailed experimental data of Friedman and Ross.⁴ We found that only one of the two regions acceptable at 3.0 GeV/c could fit the 2.64-GeV/c K^{*-} data, and the Friedman and Ross letter reports that a good fit could only be obtained for region II, with (ξ, η) near $(-1.8, -1.1)$. The conclusion that only one region can fit the data is correct, but because of an error on our part, the preferred value should be $(1.8, 1.1)$ and region I is chosen.

The consequences of this error have led to some absorption-model predictions concerning the behavior of K^{*+} production compared to K^{*-} , and we present a complete discussion of the problem. In Sec. II the choice of couplings and the method of calculation are described. The 2.64-GeV/c K^{*-} data are used to obtain couplings in Sec. III, and the comparison between model and experiment is shown. Similarly in Sec. IV the $K^{*\pm}$ data at 3.0 GeV/c are considered, and a comparison of the K^{*+} versus K^{*-} results is made, along with absorption-model predictions for both. We discuss in Sec. V the possibility of determining the ρ and ω exchange contributions separately by studying reactions with neutral K^* production or reactions on deuterium. In Sec. VI a comparison with $SU(6)$ predictions for the couplings is made, and predictions for high energies and other re-

* Supported by the U. S. Office of Naval Research under Contract N00014-67-A-0305-0005.

† Presently National Science Foundation Postdoctoral fellow, Theoretical Studies Division, CERN, Geneva, Switzerland.

¹ S. Goldhaber, *Proceedings of the Athens Topical Conference on Recently Discovered Resonant Particles*, edited by B. A. Munir and L. J. Gallagher (Ohio University Press, Athens, Ohio, 1963), p. 92.

² S. Goldhaber, J. L. Brown, I. Butterworth, G. Goldhaber, A. A. Hirata, J. A. Kadyk, and G. H. Trilling, *Phys. Rev. Letters* **15**, 737 (1965).

³ G. W. London, R. R. Rau, N. P. Samios, S. S. Yamamoto, M. Goldberg, S. Lichtman, M. Primer, and J. Leitner, *Phys. Rev.* **143**, 1034 (1966).

⁴ J. H. Friedman and R. R. Ross, *Phys. Rev. Letters* **16**, 485, 832(E) (1966).

⁵ W. P. Trower and J. R. Ficenec, *Bull. Am. Phys. Soc.* **11**, 767 (1966).

⁶ G. R. Lynch, M. Ferro-Luzzi, R. George, Y. Goldschmidt-Clermont, V. P. Henri, B. Jongejans, D. W. G. Leith, F. Muller, and J.-M. Perreau, *Phys. Letters* **9**, 359 (1964); M. Ferro-Luzzi, R. George, Y. Goldschmidt-Clermont, V. P. Henri, B. Jongejans, D. W. G. Leith, G. R. Lynch, F. Muller, and J.-M. Perreau, *Nuovo Cimento* **36**, 1101 (1965).

⁷ R. Barloutaud, A. Leveque, C. Loudec, J. Meyer, P. Schlein, A. Verglas, J. Badier, M. Demoulin, J. Goldberg, B. P. Gregory, P. Krejbich, C. Pelletier, M. Ville, E. S. Gelsema, J. Hoogland, J. C. Kluyver, and A. G. Tenner, *Phys. Letters* **12**, 352 (1964).

⁸ K. Gottfried and J. D. Jackson, *Nuovo Cimento* **33**, 735 (1964).

⁹ J. D. Jackson, J. T. Donohue, K. Gottfried, R. Keyser, and B. E. Y. Svensson, *Phys. Rev.* **139**, B428 (1965). Hereafter referred to as JDGKS.

actions are given. A brief discussion of the usefulness of our results appears in Sec. VII.

II. COUPLINGS AND ABSORPTION-MODEL DETAILS

The basic statement of the absorption model, as presented by Gottfried and Jackson⁸ and used in JDGKS, is that the partial-wave amplitude for the reaction $i \rightarrow f$ is

$$M_{fi}^j = (S_{ff}^j)^{1/2} B_{fi}^j (S_{ii}^j)^{1/2}, \quad (1)$$

where S is the S matrix and B_{fi} is the single-particle-exchange amplitude for the reaction. The calculations presented here were made using the exact partial-wave formalism,^{10,11} while those in JDGKS used an impact-parameter representation for the amplitudes. For the processes considered in this paper the differences between the two methods of calculation are less than 10%, so that the comparison with experiment is not sensitive to the method. The choice for the S -matrix elements S^j is $1 - C \exp(-\gamma(j - \frac{1}{2})^2)$, where C and γ are defined in JDGKS. As in JDGKS, the final state $\gamma_f = \frac{3}{4}\gamma_i$ and $C_f = 1.0$.

The single-particle-exchange amplitudes are calculated using perturbation theory, and correspond to the Feynman graph in Fig. 1. These amplitudes and the notation are given by Jackson and Pilkuhn.¹² In order to fix the sign of the pion and vector couplings we present the Lagrangians used to obtain the Born amplitudes:

$$\mathcal{L}_{K^*K\pi} = ig_{K^*K\pi} (K_\mu^{*+} K^+ \partial_\mu \pi^0 - \text{H.c.}), \quad (2a)$$

$$\mathcal{L}_{K^*K\rho} = i(f_{K^*K\rho} / m_{K^*}) \times (\epsilon_{\mu\nu\rho\sigma} K_\sigma^{*+} \partial_\nu K^+ \partial_\rho V_\mu^0 - \text{H.c.}), \quad (2b)$$

$$\mathcal{L}_{pp\pi} = -iG_{pp\pi} (\bar{\psi}_p \gamma_5 \psi_p) \pi^0, \quad (2c)$$

$$\mathcal{L}_{ppV} = -i\bar{\psi}_p (G_{ppV} \gamma_\mu V_\mu^0 + i(G_{ppV}^T / 2m_p) \sigma_{\mu\nu} \partial_\nu V_\mu^0) \psi_p. \quad (2d)$$

Using these one obtains the Born amplitudes for K^{*+} and K^{*-} production:

$$B_{K^{*+}} = g_{K^*K\pi} G_{pp\pi} (B^\pi + xB^V + yB^T), \quad (3a)$$

and

$$B_{K^{*-}} = g_{K^*K\pi} G_{pp\pi} (B^\pi - xB^V - yB^T), \quad (3b)$$

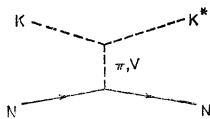


FIG. 1. Feynman graph used to obtain Born amplitudes, as in Ref. 12.

¹⁰ H. Högaasen, J. Högaasen, R. Keyser, and B. E. Y. Svensson, *Nuovo Cimento* **42**, 323 (1966).

¹¹ J. T. Donohue, Ph.D. thesis, University of Illinois, 1967 (unpublished).

¹² J. D. Jackson and H. Pilkuhn, *Nuovo Cimento* **33**, 906 (1964); **34**, 1834E (1964).

where

$$x = \frac{G_{ppV}^V f_{K^*K^+\pi^0}}{G_{pp\pi} g_{K^*K^+\pi^0}},$$

$$y = \frac{G_{ppV}^T f_{K^*K^+\pi^0}}{G_{pp\pi} g_{K^*K^+\pi^0}},$$

and $B^{\pi,V,T}$ are the amplitudes for pion exchange, and vector exchange with Dirac (vector) and Pauli (tensor) couplings to the proton, respectively. In terms of the parameters (ξ, η) in JDGKS we have

$$x = 2\xi - \eta, \quad (4a)$$

$$y = \eta. \quad (4b)$$

The difference in sign between the pion- and vector-meson-exchange contributions to K^{*-} compared to K^{*+} is a consequence of the charge-conjugation properties of

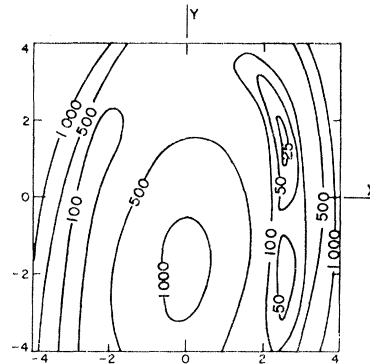


FIG. 2. Contour map of χ^2 in the (x, y) plane for fit to $K^-p \rightarrow K^{*-}p$ differential cross sections at 2.64 GeV/c, using the data of Ref. 4. Sixteen data points covering $1 \geq \cos\theta \geq -0.35$ were included. The pion couplings are $g_{K^*K\pi}^2/4\pi = 0.75$, $G_{pp\pi}^2/4\pi = 14.6$. The absorption parameters are $\gamma_i = 0.065$, $\gamma_f = 0.049$, $C_i = 0.7$, $C_f = 1.0$.

the exchanged particles, the pion being even under C , the ρ , ω , and φ being odd. In the Born approximation, even with form factors, the pion and vector-meson exchanges do not interfere, and the K^{*+} and K^{*-} reactions are predicted to be identical. In the absorption model the contributions do interfere, and K^{*+} predictions differ from K^{*-} . This difference in sign between K^{*+} and K^{*-} contributions was overlooked in JDGKS, and the error was still undetected when our analysis of the Friedman-Ross experiment was done. Since that experiment was on K^{*-} , our quoted results are wrong by the above mentioned sign. The favored values are thus (1.8, 1.1) for (ξ, η) , and region I is preferred.

III. METHOD OF SEARCH AND APPLICATION TO $K^-p \rightarrow K^{*-}p$ AT 2.64 GeV/c

The absorption-model amplitudes for $K^{*\pm}$ production, expressed in terms of the unknown quantities x

and y , are

$$M_{K^{*+}} = g_{K^{*+}K^+\pi} G_{pp\pi} (M^\pi + xM^V + yM^T),$$

$$M_{K^{*-}} = g_{K^{*-}K^+\pi} G_{pp\pi} (\tilde{M}^\pi - x\tilde{M}^V - y\tilde{M}^T),$$

where the $M^{\pi,V,T}$ are obtained from the $B^{\pi,V,T}$ via the absorption-model formula Eq. (1). The \tilde{M} differ from M only in that the absorption parameters for K^-p are different from those for K^+p . With this form the predicted cross section is quadratic in (x,y) , and χ^2 , defined by

$$\chi^2 = \sum \left\{ \left[\left(\frac{d\sigma}{d\Omega} \right)_{\text{th}} - \left(\frac{d\sigma}{d\Omega} \right)_{\text{exp}} \right] / \Delta\sigma \right\}^2, \quad (5)$$

is a fourth-order polynomial in (x,y) . In order to find (x,y) values corresponding to low χ^2 we make a contour map of χ^2 in the (x,y) plane. In view of the uncertainties and assumptions in our procedure, it seems better to delineate a region of good fit rather than giving a best value of (x,y) .

The experimental data of Friedman and Ross on the reaction $K^-p \rightarrow K^{*-}p$ ($\bar{K}^0\pi^-p$) at 2.64 GeV/c consist of the differential cross-section and the density matrix elements measured in 16 production angle bins. In Fig. 2 the χ^2 contour map made using the differential cross-section data is shown. With two degrees of freedom a χ^2 of order 20 denotes a good fit. From the map it is apparent that there are two "valleys" in the (x,y) plane with $\chi^2 < 100$, situated approximately at $x = \pm 2.5$. These correspond to regions I and II, respectively, of JDGKS. Only for $x \approx 2.5$ (Region I) does χ^2 approach the expected value.

It is apparent from the map that the fit to the differential cross section, while fairly selective on x , is permissive in y values. By comparing the theoretical and experimental density matrix elements, however, the size of the allowed region in y can be reduced. The experimental density matrix elements are in better agreement with the predictions of the $x \approx 2.5$, $y > 0$ region than with the $x \approx 2.5$, $y < 0$ region. Although the density matrix elements were not used in the χ^2 search, they were used to discriminate between parts of those regions which gave good fits to the differential cross section. It was found that in the region where χ^2 was ≈ 25 , the fit to the density matrix elements was also good, although some variation in the predicted density matrix elements occurred. In Figs. 3, 4(a), and 4(b) are displayed the experimental results of Friedman and Ross, together with our predictions using two sets of (x,y) values from the region of low χ^2 . The solid curves (a) correspond to $(x,y) = (2.5, 1.1)$, and appeared in the Friedman and Ross letter. The dashed curves (b) correspond to $(x,y) = (2.05, 1.5)$, and while the fit to the differential cross section is not as good as for (a), the density-matrix predictions are somewhat better. These curves are indicative of the changes resulting from small changes in (x,y) .

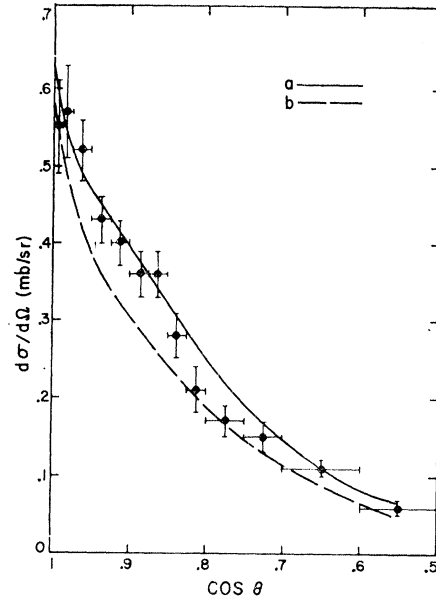


FIG. 3. The differential cross-section data on $K^-p \rightarrow K^{*-}p$ ($\bar{K}^0\pi^-p$) at 2.64 GeV/c, from Ref. 4, along with the absorption-model predictions. The curve (a) is for $(x,y) = (2.5, 1.1)$ while curve (b) is for $(x,y) = (2.05, 1.5)$. The absorption parameters are as given in Fig. 2.

The χ^2 contour map, Fig. 2, shows a local minimum at $x \approx -2.5$ corresponding to destructive interference between pion and vector-meson exchange. The interference effect is most apparent at small angles [$\cos\theta > 0.9$], where the pion and vector-meson-exchange contributions are comparable. At larger angles the pion-exchange contribution is small compared to vector-meson exchange, and the interference is less important; the parameters (x,y) and $(-x, -y)$ give similar predictions for the cross section and density matrix. Thus the region with $\chi^2 < 100$ for $x \approx -2.5$ is a reflection of the good fit obtained at wide angles for $x \approx 2.5$. Because the relative sign of the pion and vector-meson exchange contributions is opposite for $K^{*+}p$ relative to $K^{*-}p$, the $x \approx -2.5$ region should be typical of $K^+p \rightarrow K^{*+}p$. However, as pointed out in JDGKS, the absorption parameters for K^+p and K^-p are different at energies ~ 3 GeV/c, and this will have some effect on the model predictions. In Figs. 5(a) and 5(b) we compare predictions for $d\sigma/d\Omega$ and ρ_{00} in $K^{*-}p$ and $K^{*+}p$ at 2.64 GeV/c, using $(x,y) = \pm(2.5, 1.1)$.

The curves are:

Fig.	Curves	Reaction	(x,y)
5(a)	solid	K^{*-}	(2.5, 1.1)
	dashed	K^{*+}	(-2.5, -1.1)
5(b)	solid	K^{*+}	(2.5, 1.1)
	dashed	K^{*-}	(-2.5, -1.1).

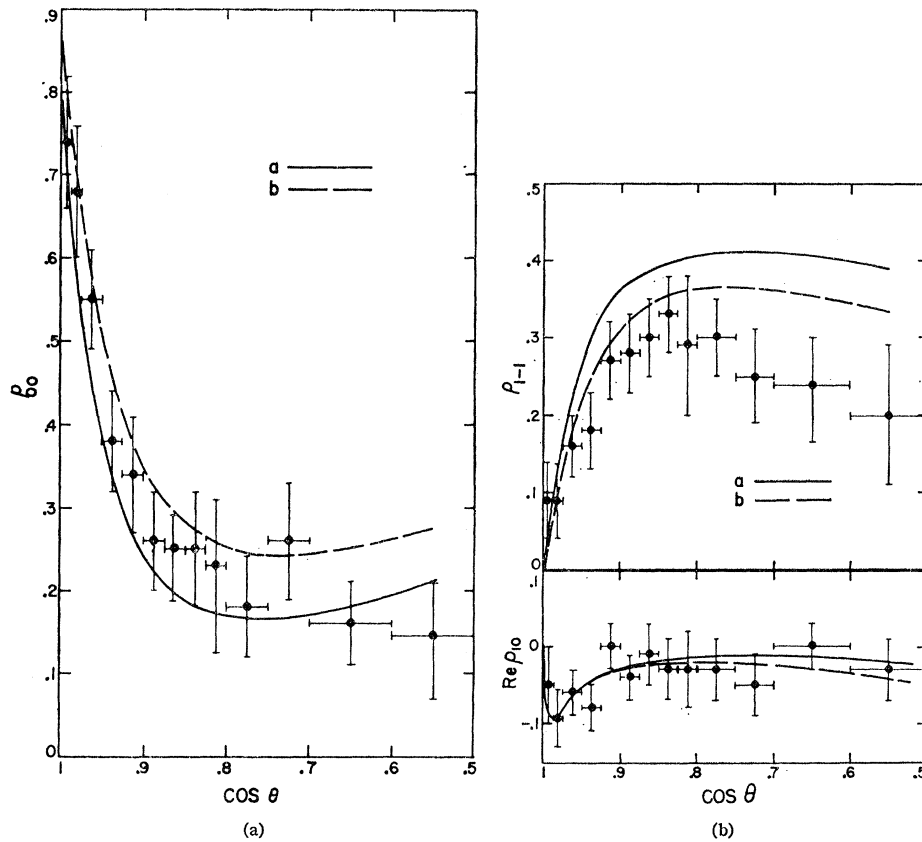


FIG. 4. The density matrix for $K^-p \rightarrow K^{*-}p$ at 2.64 GeV/c. The data and absorption-model curves are as in Fig. 3. (a) shows ρ_{00} while (b) gives ρ_{1-1} and $\text{Re } \rho_{10}$.

The absorption parameters are:

$$K^-p: \gamma_i=0.065, \gamma_f=0.049, C_i=0.7, C_f=1.0,$$

$$K^+p: \gamma_i=0.13, \gamma_f=0.097, C_i=0.93, C_f=1.0.$$

With this presentation the effects both of the interference and the different absorption parameters are apparent. Figure 5(a) shows constructive interference between pion and vector-meson exchange; the solid and dashed curves differ only by the absorption parameters used. In Fig. 5(b) destructive interference is shown, the solid and dashed curves again corresponding to different absorption. The solid curves are our choices for $K^-p \rightarrow K^{*-}p$ [Fig. 5(a), constructive interference] and $K^+p \rightarrow K^{*+}p$ [Fig. 5(b), destructive interference]; the dashed curves correspond to opposite signs for (x,y) .

The significant features of the interplay between interference and different absorption parameters, as shown in Fig. 5, are the following:

(1) The interference effect causes $d\sigma/d\Omega$ to round off near $\theta=0^\circ$ for destructive interference, while peaking for constructive.

(2) The density matrix element ρ_{00} displays similar behavior, being larger near $\theta=0^\circ$ for constructive interference.

(3) Changing the absorption parameters produces an appreciable change of size in $d\sigma/d\Omega$, but only a very small effect in ρ_{00} .

(4) The approximate equality of K^{*+} and K^{*-} cross sections (solid curves) is a consequence of both interference and different absorption parameters; the interference tends to suppress K^{*+} relative to K^{*-} , but the weaker absorption in K^{*+} tends to produce a larger cross section. These opposing tendencies largely cancel each other and the total K^{*+} cross section is approximately equal to that for K^{*-} , although $d\sigma/d\Omega$ has a different shape.

The data on K^{*-} at 2.64 GeV/c clearly favor the $x \approx 2.5$ region, on the basis of features (1) and (2). Also the approximate equality of K^{*+} and K^{*-} cross sections supports our contention of constructive interference for K^{*-} , and destructive for K^{*+} . As seen from Fig. 5, the choice $x \approx -2.5$ would require a K^{*+} cross section almost twice as big as K^{*-} .

The insensitivity of the density matrix to the absorption parameters means that the changes in absorption affect the scale of the amplitudes, but do not greatly alter the relative strengths. In terms of the contour map in Fig. 2, a small change in the absorption parameters produces shifts in the contour lines, but does not strongly affect the over-all picture. The two valleys of low χ^2 persist, corresponding to constructive and destructive interference.

Since in the limit of no absorption the interference effect disappears, it is clear that interference and absorption are correlated. Nevertheless, at energies near

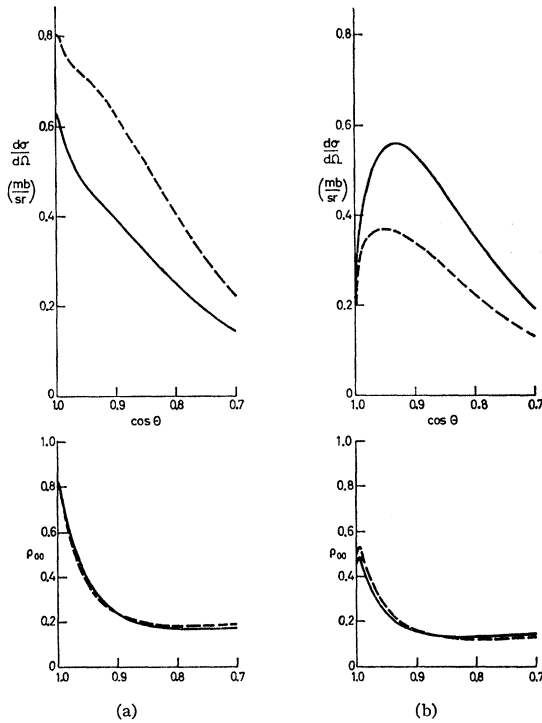


FIG. 5. Absorption-model calculations for $d\sigma/d\Omega$ and ρ_{00} for $K^\pm p \rightarrow K^{*\pm} p$ at 2.64 GeV/c, with $(x,y) = \pm(2.5, 1.1)$. The absorption parameters for K^-p are as in Fig. 2, while for K^+p , $\gamma_i = 0.13$, $\gamma_f = 0.097$, $C_i = 0.93$, $C_f = 1.0$. (a) shows K^{*-} with $(x,y) = (2.5, 1.1)$ (solid curves), and K^{*+} with $(x,y) = (-2.5, -1.1)$ (dashed curves). (b) shows K^{*+} with $(x,y) = (2.5, 1.1)$ (solid curves), and K^{*-} with $(x,y) = (-2.5, -1.1)$ (dashed curves).

3 GeV/c, the peaking effect we attribute to constructive interference cannot be deformed, by modest changes in the absorption parameters, into the rounding effect characteristic of destructive interference. The same is true for the behavior of ρ_{00} near small angles.

IV. $K^{*\pm}$ PRODUCTION AT 3.0 GeV/c

Armed with the results obtained at 2.64 GeV/c we attempt to fit the experimental results on $K^\pm p \rightarrow K^{*\pm} p$ at 3.0 GeV/c.^{6,7} The incorrect energy dependence of vector-meson exchange will produce a shift in the region of best χ^2 compared to 2.64 GeV/c, but because the energy difference is small, the shift is not large. Using Eq. (5) we search for (x,y) values near region I which give good fits to both K^{*+} and K^{*-} data. As explained in Sec. III, the differences in predictions between (x,y) and $(-x, -y)$ are confined to small production angles, e.g., $\cos\theta > 0.9$. There is, however, the effect of different absorption parameters for K^+p and K^-p , so that even at large production angles there is some difference between K^{*+} and K^{*-} cross sections. Still the basic prediction holds that K^{*+} and K^{*-} cross sections and density matrices should be similar at large production angles and be different at small angles.

In Figs. 6 and 7 are shown the cross-section data for

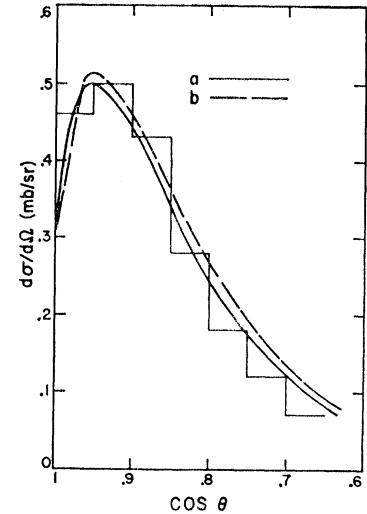


FIG. 6. The differential cross section for $K^+p \rightarrow K^{*+}p$ ($K^{0\pi^+}p$) at 3.0 GeV/c, as given in Ref. 6. The absorption-model curves are made using absorption parameters $\gamma_i = 0.11$, $\gamma_f = 0.083$, $C_i = 0.9$, $C_f = 1.0$. Curve (a) is for $(x,y) = (2.05, 1.5)$, curve (b) for $(x,y) = (2.1, 0.95)$.

$K^{*\pm}$, together with theoretical predictions, (a) with $(x,y) = (2.05, 1.5)$ and (b) with $(2.1, 0.95)$. The K^{*+} differential cross section apparently does round off in the forward direction, in agreement with the absorption-model predictions. From the K^{*-} data it is difficult to test the predictions, as the bin size is so large, but it is clear that a reasonable fit is obtained to both K^{*+} and K^{*-} cross sections using the same (x,y) values. The predictions of the absorption model for the $K^{*\pm}$ density matrix also reflect the interference between pion and vector-meson exchange. In Table I the averaged density-matrix predictions for the indicated angular intervals are presented, along with the experimental values. The agreement between experiment and theory for the (x,y) choices (a) and (b) is reasonable, the predicted values usually falling within the error estimates. While the predictions for ρ_{00} in the first $\cos\theta$ bin are slightly greater than the experimental values, they resemble experiment in that ρ_{00} for K^{*-} is larger than that for K^{*+} . This is caused by the interference between pion

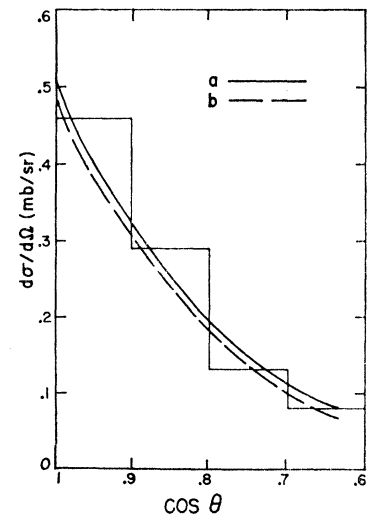


FIG. 7. The differential cross section for $K^-p \rightarrow K^{*-}p$ ($\bar{K}^0\pi^-p$) at 3.0 GeV/c, as given in Ref. 7. The curves (a) and (b) have the same (x,y) values as in Fig. 6, but the absorption parameters are $\gamma_i = 0.05$, $\gamma_f = 0.037$, $C_i = 0.64$, $C_f = 1.0$.

TABLE I. Comparison of theoretical and experimental density-matrix elements for K^{*-} and K^{*+} at 3.0 GeV/c.

	$\langle\rho_{00}\rangle$	$\langle\rho_{1,-1}\rangle$	$\langle\text{Re}\rho_{10}\rangle$
K^{*-} density matrix. (3.0 GeV/c)			
0.9 < $\cos\theta$ < 1.0			
Exp. ^a	0.34±0.08	0.35±0.06	0.01±0.04
(a)	0.48	0.23	-0.03
(b)	0.46	0.23	-0.04
0.8 < $\cos\theta$ < 0.9			
Exp. ^a	0.10±0.09	0.33±0.08	-0.01±0.05
(a)	0.24	0.37	-0.02
(b)	0.18	0.40	-0.02
K^{*+} density matrix. (3.0 GeV/c)			
0.925 < $\cos\theta$ < 1.0			
Exp. ^b	0.15±0.11	0.23±0.09	-0.06±0.06
(a)	0.16	0.28	-0.06
(b)	0.22	0.28	-0.06
0.825 < $\cos\theta$ < 0.925			
Exp. ^b	0.14±0.09	0.40±0.07	-0.03
(a)	0.10	0.43	-0.03
(b)	0.12	0.43	-0.03

^a From Ref. 7.^b From Ref. 6.

and vector-meson exchange at small angles, for K^{*-} constructive and favoring the larger ρ_{00} value.

On the basis of the agreement between absorption-model predictions and experiment at 2.64 and 3.0 GeV/c we may argue that the model with vector-meson exchange can be used to obtain meaningful results. In particular, the prediction of interference between pion and vector-meson exchange appears to be borne out, although a confirmation of the rounding of K^{*+} cross sections near $\cos\theta=1$ would be useful. The region of best (x,y) values, for the energy range 2.6 to 3.0 GeV/c, is found to be

$$x = 2.3 \pm 0.3,$$

$$y = 0.5 \text{ to } 2.0.$$

The pion coupling constants used are

$$g_{K^{*+}K^+\pi^0}/4\pi = 0.75, \quad G_{pp\pi^0}/4\pi = 14.6.$$

V. POSSIBLE DETERMINATION OF ρ AND ω EXCHANGE CONTRIBUTIONS

The quantities (x,y) are actually sums of couplings for ρ , ω , and φ , i.e.,

$$x = x_\rho + x_\omega + x_\varphi, \quad (6)$$

and

$$y = y_\rho + y_\omega + y_\varphi.$$

Assuming that the φ contribution is negligible, we can in principle determine (x_ρ, y_ρ) from an analysis of neutral K^* production. Data obtained using neutrons as target particles also can be used to separate the ρ and ω contributions, since the ρ and ω have different isotopic spin. For the six possible $KN \rightarrow K^*N'$ reactions we can

write the Born amplitudes in the form

$$B_i = N_i g_{K^{*+}K^+\pi^0} G_{pp\pi^0} (B^\pi + x_i B^V + y_i B^T). \quad (7)$$

The quantities x_i, y_i depend on $x_\rho, x_\omega, y_\rho, y_\omega$, as shown in Table II. To each reaction corresponds a different combination of exchanges, so that the absorption-model predictions for each reaction will be different. In principle, by analyzing one of the reactions (3)–(6), together with the results obtained from reactions (1) and (2), one can determine (x_ρ, y_ρ) and (x_ω, y_ω) and predict the behavior of the remaining three reactions.

There exist data on the neutral K^* reactions (3) and (4). In a K^+d experiment at 2.3 GeV/c both reaction (1) and reaction (4) were observed.² The production and decay distributions for the two reactions were clearly different, and it was concluded that the latter was consistent with pion exchange alone. Hence the vector-meson exchange in $K^{*+}p$ was concluded to be isoscalar, and assuming no appreciable φ exchange, the ω was the exchanged meson.

The reaction $K^-p \rightarrow \bar{K}^{*0}n$ ($K^-\pi^+n$), has been studied by Trower and Ficeneç⁵ at 2.67 GeV/c in an analysis of the two-prong events in the same exposure used by Friedman and Ross.⁴ At present only preliminary data are available, and the error estimates permit a large range of acceptable fits. The cross section and density matrix observed are found to be consistent with pion exchange alone, in agreement with the results on reaction (5). However, in this case it is not possible to rule out a small amount of vector-meson exchange. The experimental data are not precise enough to permit an analysis such as was done for K^{*-} , but an estimate of the permissible ρ exchange can be found by searching along the line $y_\rho = 3.7x_\rho$ in the (x_ρ, y_ρ) plane. This corresponds to the ratio $(G_{pp\rho^T}/G_{pp\rho^V}) = 3.7$, which is obtained from electromagnetic form factors. We find that for $x_\rho = 0.2$ the fit is as good as pion exchange alone, and in view of the experimental uncertainties, x_ρ could be as large as 0.4. While these values of x_ρ are small compared to the value of 2.2 for $(x_\rho + x_\omega)$ obtained for reactions (1) and (2), the corresponding y_ρ values of 0.7 to 1.4 are comparable to the range 0.5 to 2.0 for $(y_\rho + y_\omega)$. Hence a plausible decomposition into (x_ρ, y_ρ) and (x_ω, y_ω) is

$$x_\rho \simeq 0.2 \pm 0.2, \quad x_\omega \simeq 2.0 \pm 0.4,$$

$$y_\rho \simeq 0.7 \pm 0.7, \quad y_\omega \simeq 0.5 \pm 0.5.$$

If one assumes that the φNN couplings are negligible, such a decomposition is compatible with the result from the isoscalar electromagnetic form factors $(G^T/G^V)_{\text{isoscalar}} \simeq 0$. Reactions (5) and (6) are difficult to analyze, since they require a deuterium target and have a neutron in the final state, but they would provide a test of the decomposition of x into x_ρ and x_ω . In particular the tensor coupling, which for these reactions depends on $(y_\rho - y_\omega)$, should be small compared to the $K^\pm p$ reactions, as the latter depend on $(y_\rho + y_\omega)$. If we

use observations that cross sections do not depend strongly on y , and that $x_\rho \ll x_\omega$, we can predict that the cross section for the reaction $K^{*+}n$ will resemble $K^{*-}p$, while that for $K^{*-}n$ will be similar to $K^{*+}p$. In terms of the shape of the forward peak, $K^{*+}n$ should peak up while $K^{*-}n$ should round off.

VI. EXTENSIONS OF THE MODEL

If one accepts the successful fitting of the K^{*-} data at 2.6 GeV/ c and the comparison of K^{*+} with K^{*-} production at 3 GeV/ c as evidence for the validity of the absorption model using a mixture of pion and vector-meson exchange, there are several questions which can be asked to test or extend the model. Three such questions, which we attempt to answer, are: How do the results compare with symmetry predictions? What happens at higher energies? What other reactions might provide evidence for a mixture of pseudoscalar and vector-meson exchange?

A. Comparison of Couplings with Relativistic $SU(6)$ Predictions

The couplings we obtain by fitting the data near 3 GeV/ c may be compared with the relativistic $SU(6)$ couplings given by Sakita and Wali.¹³ In their paper the couplings of the 0^- , 1^- , $\frac{1}{2}^+$, and $\frac{3}{2}^+$ multiplets are expressed in terms of two parameters, one for trilinear-meson couplings, the other for meson-baryon couplings. Since we take the $K^+\pi^0 K^{*+}$ and $p\bar{p}\pi^0$ couplings as known, these two parameters are fixed and the ρ , ω , and φ couplings are predicted. We assume, in agreement with the symmetry predictions, that the φ -meson coupling to the nucleons is weak, and take only ω and ρ . If we follow our convention for the Lagrangians, which differs by a sign from the VVP coupling of Sakita and Wali, we obtain the symmetry predictions, in the limit of low-momentum transfer:

$$x_\rho/x_\omega = \frac{1}{3}, \quad (8a)$$

$$y_\omega/x_\omega \simeq 0.15, \quad (8b)$$

$$x_\omega \simeq -1, \quad (8c)$$

$$y_\rho/x_\rho \simeq 4.7. \quad (8d)$$

In decomposing the vector-meson exchange into ρ and ω contributions we used a condition similar to (8d) above, and thus can compare our results only with predictions (8a), (8b), and (8c). We find from our fitting procedure

$$x_\rho/x_\omega \simeq 0.1, \quad (9a)$$

$$y_\omega/x_\omega \simeq \frac{1}{4}, \quad (9b)$$

$$x_\omega \simeq 2. \quad (9c)$$

Our results are roughly consistent with (a) and (b), but

¹³ B. Sakita and K. C. Wali, Phys. Rev. **139**, B1355 (1965).

for (c) there is a disagreement in sign.¹⁴ In our model the sign of x_ω is determined by the character of the interference between pion and vector-meson exchange, and we cannot obtain a good fit to the Friedman and Ross K^{*-} data at small angles using a negative sign for x_ω . The absorption model is certainly not sufficiently well founded to provide a definitive test of the signs of symmetry predictions. All we can say is that with our version of the absorptive peripheral model and taking the relative sign of pion and vector-meson exchange from relativistic $SU(6)$, one predicts constructive interference in K^{*+} and destructive interference in K^{*-} , in contradiction to the experimental results at momenta $\simeq 3$ GeV/ c .

B. Energy Dependence of K^*N Reactions

There are several recent experiments observing $K^\pm p \rightarrow K^{*\pm} p$ at incident momenta from 3.5 to 13 GeV/ c .¹⁵ None of these have as yet the high statistics of the Friedman and Ross experiment. Hence while they measure the general features of the differential cross section and density matrix elements, fine details, such as momentum-transfer dependence at small angles, are not so well determined. The gross features appear to be relatively independent of the incident energy, apart from the decrease with energy of the total cross section. The average values of density matrix elements for $K^+p \rightarrow K^{*+}p$ are found to be equal, within errors, at 3.0, 3.5, and 5.0 GeV/ c .^{15a} Charged K^* decay angular distributions display a strong $\cos 2\varphi$ term, corresponding to $\langle \rho_{1,-1} \rangle \simeq 0.4$, at all energies. But the \bar{K}^{*0} decay angular distribution at 10 GeV/ c does not show strong evidence for vector exchange, in agreement with experiments at low energies.¹⁶ Hence pion exchange may be a dominant

¹⁴ A small value for the ρ -exchange contribution is suggested by the A -parity quantum number of Bronzan and Low, Phys. Rev. Letters **12**, 522 (1964). The $\rho K K^*$ coupling is forbidden if A parity is a good quantum number.

¹⁵ A partial list of such experiments is: (a) 3.5 and 5.0 GeV/ c K^+p : Brussels-CERN Collaboration, W. De Baere *et al.*, Nuovo Cimento **51**, 401 (1967); (b) 4.1 and 5.5 GeV/ c K^-p : F. Schweingruber *et al.*, Bull. Am. Phys. Soc. **12**, 46 (1967); F. Schweingruber, Ph.D. thesis, Northwestern University, 1967 (unpublished). In the latter it is shown that a good fit to the K^{*-} differential cross section and density matrix at 5.5 GeV/ c is obtained by D. Griffiths and R. Jabbur. The absorption model is used with the $SU(6)$ prediction for $x (\simeq -1)$ and $y=0$. This is in contrast to our result of a positive x value, based on low-energy data. The disagreement is essentially confined to the behavior of ρ_{00} at small angles [$\cos\theta \geq 0.98$, $\Delta^2 \leq 0.05$ (GeV/ c)²] where our prediction [Fig. 9(a), solid curve] is larger than this experimental result. For $0 \leq \Delta^2 \leq 0.1$ (GeV/ c)², $\langle \rho_{00} \rangle = 0.28 \pm 0.07$ experimentally, while our prediction for $(x,y) = (1.0,0.5)$ is $\langle \rho_{00} \rangle \simeq 0.5$. In order to resolve the question of the sign of x , precise measurements of ρ_{00} at small angles are required, and K^{*+} and K^{*-} results should be compared; (c) 6.0 GeV/ c K^-p : British University Collaboration (unpublished); (d) 10 GeV/ c K^-p : Aachen-Berlin-CERN-London (I.C.) Collaboration (unpublished); (e) 13 GeV/ c K^+p : A. C. Melissinos *et al.*, Bull. Am. Phys. Soc. **12**, 46 (1967).

¹⁶ Preliminary results of Aachen-Berlin-CERN-London (I.C.) collaboration on K^-p at 10 GeV/ c (private communication). See also rapporteur's paper, J. D. Jackson, in *Proceedings of the XIIIth International Conference on High Energy Physics* (University of California Press, Berkeley, 1967), esp. pp. 157-158.

mechanism in neutral K^* production even at high energies. From these general features one may conclude that the production mechanism is relatively independent of the incident energy.

This picture of insensitivity to energy may be changed when the details of K^* production are observed. For example, the question of interference between exchange contributions can be resolved only by precise measurements of $d\sigma/d\Omega$ and ρ_{00} in small angular intervals near the forward direction. Because this possible interference effect is confined to a small angular region, it does not contribute much to the averaged values of quantities. Hence it is conceivable that the details of the experiment may be sensitive to the incident energy, even though the gross features are not. Until sufficient data are accumulated, the question of energy dependence remains partially open.

While the K^*N production mechanism may be approximately energy-independent, absorption-model predictions using a mixture of pion and vector-meson exchange are very sensitive to energy. The pion-exchange contribution seems to have a reasonable energy dependence, since it agrees approximately with neutral K^* data at 2.3 and 10 GeV/c. The vector-meson-exchange predictions fail at high incident momenta in both energy- and momentum-transfer dependence. We circumvent the energy-dependence problem phenomenologically by using different couplings at different energies, but the momentum-transfer problem, that the predicted cross sections are too broad in angle, remains. While some variation in the shape of $d\sigma/d\Omega$ can

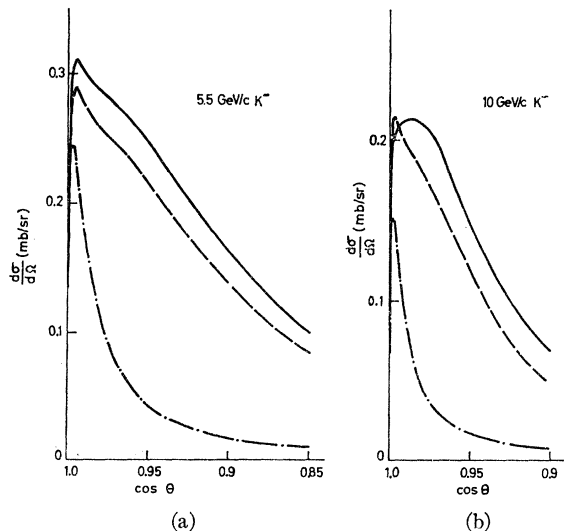


FIG. 8. Differential cross-section predictions of the absorption model for $K^-p \rightarrow K^*p$ ($\bar{K}^0\pi^-p$). (a) is for 5.5-GeV/c momentum K^- . The absorption parameters are $\gamma_i=0.024$, $\gamma_f=0.018$, $C_i=0.52$, $C_f=1.0$. The solid curve is for $(x,y)=(1.0,0.5)$, the dashed curve for $(-1.0,-0.5)$, and the dash-dotted curve for pion exchange. (b) is for 10 GeV/c K^- . The absorption parameters are $\gamma_i=0.016$, $\gamma_f=0.012$, $C_i=0.48$, $C_f=1.0$. The solid curve is for $(x,y)=(0.5,0.3)$, the dashed curve for $(-0.5,-0.3)$, and the dash-dotted curve is for pion exchange.

be made by changing (G_{ppV^0T}/G_{ppV^0V}) , the experimental cross-section data at 10 GeV/c cannot be fitted.¹⁶ This applies only for calculations made using the recipe for absorption given in JDGKS. The inclusion of form factors or stronger absorption of low partial waves could produce agreement, but the significance of such agreement would be reduced because of the additional arbitrariness in the model.

We have investigated the predictions of the absorption model at various high energies, choosing couplings so that the cross section predicted by vector-meson exchange is about four times as large as that of pion exchange. This was done by taking the quantity x pro-

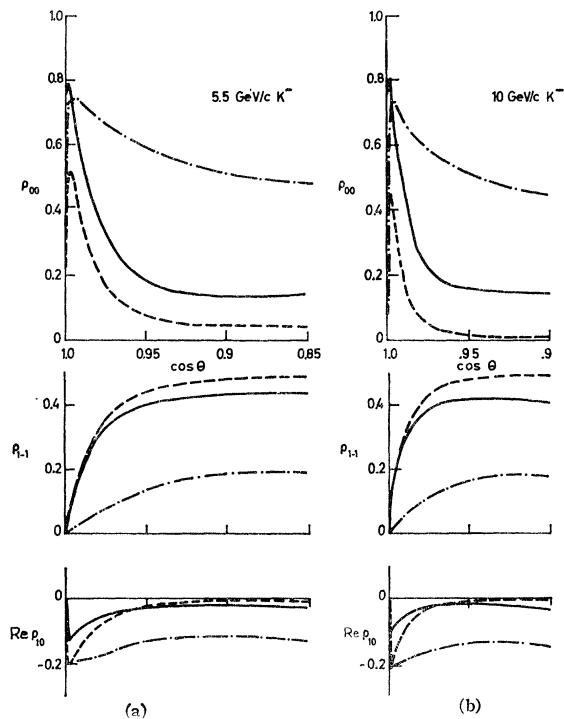


FIG. 9. Density-matrix predictions for $K^-p \rightarrow K^*p$. The curves are as described in Fig. 8. (a) gives the predictions at 5.5 GeV/c, while (b) gives the 10-GeV/c results.

portional to P_{lab}^{-1} , where P_{lab} is the incident beam momentum. The object was to study qualitatively the predicted interference effects at various energies. We show in Figs. 8 and 9 some absorption-model calculations for $K^-p \rightarrow K^*p$ at 5.5 and 10 GeV/c. The predicted cross sections and density matrices are shown for both constructive (solid curves) and destructive (dashed curves) interference, along with the pion-exchange contributions (dash-dotted curves). At 5.5 GeV/c we use $(x,y)=\pm(1.0,0.5)$, and at 10 GeV/c $(x,y)=\pm(0.5,0.3)$, the + sign denoting constructive interference. The absorption parameters are $\gamma_i=0.024$, $C_i=0.52$, $\gamma_f=0.018$, $C_f=1.0$ at 5.5 GeV/c, and $\gamma_i=0.016$, $C_i=0.48$, $\gamma_f=0.012$, $C_f=1.0$ at 10 GeV/c. The (G_{ppV^0T}/G_{ppV^0V}) ratio is thus $\simeq \frac{1}{2}$, as we found for the

2.6-GeV/c K^- data. The dashed curves at 5.5 GeV/c correspond roughly to the $SU(6)$ prediction of $x \simeq -1$; we favor the solid curves from our analysis of the data at lower energies.

There are three general features of these curves that are of interest:

(1) The broad angular distribution of the differential cross section for vector-meson exchange.

(2) The rounding off of the cross-section predictions near the forward direction for both signs of the interference.

(3) The absence of qualitative differences between cross-section and density-matrix predictions for constructive and destructive interference.

Only for ρ_{00} are the model predictions sensitive to the sign of the interference; a larger ρ_{00} is predicted for constructive interference. If our conclusions based on low-energy results are reliable, K^{*-} should yield a larger ρ_{00} than K^{*+} at the same incident energy. However, the predictions for ρ_{00} are moderately sensitive to the ratio (G_{ppV^0T}/G_{ppV^0V}); increasing (y/x) for fixed x tends to

TABLE II. The quantities N_i , x_i , and y_i as used in Eq. (7).

Reaction	N_i	x_i	y_i
1. $K^+p \rightarrow K^{*+}p$	1	$(x_\rho + x_\omega)$	$(y_\rho + y_\omega)$
2. $K^-p \rightarrow K^{*-}p$	1	$-(x_\rho + x_\omega)$	$-(y_\rho + y_\omega)$
3. $K^-p \rightarrow \bar{K}^{*0}n$	2	$-x_\rho$	$-y_\rho$
4. $K^+n \rightarrow K^{*0}p$	2	x_ρ	y_ρ
5. $K^+n \rightarrow K^{*+}n$	1	$(x_\rho - x_\omega)$	$(y_\rho - y_\omega)$
6. $K^-n \rightarrow K^{*-}n$	1	$-(x_\rho - x_\omega)$	$-(y_\rho - y_\omega)$

raise the solid curve and lower the dashed. Thus the interference effect in ρ_{00} should be more apparent if the tensor coupling is appreciable. We do not show any predictions for K^{*+} production since the use of different absorption parameters does not produce any significant changes. Therefore the dashed curves may be taken as typical K^{*+} predictions, with the solid curves being K^{*-} .

The principle conclusions of our investigation at higher energies are:

(1) The differential cross section predicted from vector-meson exchange is too broad in angle.

(2) The interference between pion and vector-meson exchange is no longer reflected strongly in the differential cross section, but perhaps is still present in the ρ_{00} density matrix elements for K^{*+} and K^{*-} .

(3) It is impossible to determine couplings by fitting cross-section data at high energy; for a fit only to density matrix elements, extremely precise measurements are needed even to determine the sign of the couplings.

C. Tests of Interference in Other Reactions

If, as we claim, the experimental differences between $K^{*+}p$ and $K^{*-}p$ production are caused by interference

TABLE III. Reactions which may show evidence for interference between pseudoscalar- and vector-meson exchange. Comparison of different charge states.

Reaction	Pseudoscalar-meson exchange amplitude	Vector-meson exchange amplitude
$\pi^+p \rightarrow \rho^+p$	π	$\omega(\varphi)$
$\pi^-p \rightarrow \rho^-p$	π	$-\omega(-\varphi)$
$\pi^-p \rightarrow \rho^0n$	$\sqrt{2}\pi$	
$K^+p \rightarrow K^{*0}N^{*++}$	$\sqrt{2}\pi$	$\sqrt{2}\rho$
$K^+p \rightarrow K^{*+}N^{*+}$	$(\sqrt{\frac{1}{3}})\pi$	$(\sqrt{\frac{1}{3}})\rho$
$K^-p \rightarrow \bar{K}^{*0}N^{*0}$	$(\sqrt{\frac{2}{3}})\pi$	$-(\sqrt{\frac{2}{3}})\rho$
$K^-p \rightarrow K^{*-}N^{*+}$	$(\sqrt{\frac{1}{3}})\pi$	$-(\sqrt{\frac{1}{3}})\rho$

between pseudoscalar and vector-meson exchange, other reactions should provide supporting evidence. The effect could be best observed by comparing similar reactions for which the interference occurs with opposite signs. As in Table II we can use the charge conjugation properties of the possible exchanged particles and compare different charge states of the same reaction. The reactions $\pi p \rightarrow \rho N$ and $K p \rightarrow K^* N^*$ may provide some evidence for interference: the former between π and ω , the latter between π and ρ . In Table III we give the strengths and relative signs of the couplings for these reactions, just as in Table II.

A second method of testing the interference is to compare K^-p reactions producing the neutral vector mesons ρ^0 , ω , and φ and a $Y=0$ baryon. For these three reactions the baryon vertices are identical; the relative signs and strengths of the V^0KK and V^0KK^* couplings determine the character of the interference. That is, once the nature of the interference in one reaction is known, it can be predicted for the other two. Hence we need only compare the ratios ($g_{V^0KK^*}/f_{V^0KK^*}$) for $V^0 = \varphi$, ω , and ρ^0 . These ratios are predicted by Sakita and Wali and are shown in Table IV. It should be remarked that only $SU(3)$ with $\omega - \varphi$ mixing is needed to obtain these ratios.

There is some experimental evidence available to test the existence of these interference effects. Let us recall that constructive interference gives a larger ρ_{00} than destructive interference, and that at lower momenta the differential cross section may show a peak at small angles for constructive interference, while for destructive interference a rounding off may occur. The data on

TABLE IV. Reactions in which K and K^* exchange may interfere, with $SU(6)$ predictions for the ratio $f_{V^0K^*K}/g_{V^0KK}$. (Taken from Ref. 13, neglecting mass differences.) Y can be any hypercharge 0 baryon.

Reaction	Predicted $f_{V^0K^*K}/g_{V^0KK}$
$K^-p \rightarrow \omega Y$	2
$K^-p \rightarrow \varphi Y$	-2
$K^-p \rightarrow \rho^0 Y$	-2

$K^-p \rightarrow \omega\Lambda$ and $\varphi\Lambda$ at 2.6 GeV/c¹⁷ have been studied by Flatté,¹⁸ using an absorption-model procedure similar to ours. He finds that constructive interference is preferred for the $\omega\Lambda$ data, and destructive interference for the $\varphi\Lambda$. This change in the sign of the interference is in agreement with the predictions of Table IV.

There are also some experimental data on the reactions in Table III, but no strong evidence for interference effects is present. The density-matrix and cross-section predictions for pion exchange are in reasonable agreement with experiment, as shown in JDGKS. Thus, if vector-meson exchange occurs, it is not very strong, and the interference effects are presumably weak. Recent experiments on ρ^- production at 4.2¹⁹ and 8.0 GeV/c²⁰ find some deviation from the absorption-model predictions, especially for the density matrix elements. It is found experimentally that ρ_{00} is smaller for ρ^- than for ρ^+ at similar energies, which suggests possible destructive interference in ρ^- production. Since $\omega(\varphi)$ exchange cannot occur in ρ^0 production, we suggest that the three reactions ($\pi^-p \rightarrow \rho^-p$, $\pi^-p \rightarrow \rho^0n$, $\pi^+p \rightarrow \rho^+p$) be compared at the same energies, to see if any systematic evidence for interference is present.

It is interesting to note that for $\pi p \rightarrow \rho N$ reactions, isospin conservation gives the inequality

$$d\sigma_{\rho^+} + d\sigma_{\rho^-} - d\sigma_{\rho^0} \geq 0,$$

where $d\sigma$ represents a differential cross section or a differential cross section multiplied by a diagonal density matrix element. If the isoscalar-exchange contribution is zero, the inequality becomes an equality. Hence a measurement of the left-hand side of the inequality provides a limit to the isospin-0 exchange, e.g., the ω meson, without reference to any particular model. Experimentally the ρ^0 cross section is about twice as large as the charged- ρ cross sections, so that the left-hand side is roughly consistent with being zero. A precise test of this inequality using diagonal density matrix elements would provide information on isoscalar-exchange in a model-independent manner.

VII. CONCLUSIONS

We have attempted to show that the absorption model with a mixture of pion and vector-meson exchange can explain the experimental data on K^*p

reactions in the momentum range $\sim 2-4$ GeV/c. The model uses two free parameters, which are formally identified with the vector and tensor couplings of the exchanged vector mesons. The fitting procedure requires these parameters to decrease with increasing momenta. This makes our identification rather meaningless, since coupling strengths should remain constant. Still, the model is able to describe the detailed behavior of the cross section and density matrix using only two parameters. Furthermore, the same set of parameters explains both K^{*+} and K^{*-} production, the differences between these reactions being explained by the change in sign of the parameters which stems from the different charge conjugation properties of the exchanged pion and the vector meson. Thus the model provides an economical description of K^* production.

The results we obtain are admittedly questionable, since we evade the problem of energy dependence. But they may be useful in formulating a correct theory of production mechanisms. For example, we may compare the absorption and Regge-pole models. The Regge-pole model is a theory which does not violate any basic concepts and can in principle be applied to production reactions. But the number of residue functions with unknown t dependence is large when the particles produced have high spins; this fact plus arbitrariness in trajectories makes a comparison of theory and experiment difficult.²¹ The absorption model, conversely, is not a respectable theory, since it violates unitarity, but it is easily compared with experiment, often quite successfully. If the good results of the absorption model are not accidental, it should be possible to incorporate them in a more complete theory.

ACKNOWLEDGMENTS

Much of the present work formed part of a thesis prepared under the supervision of Professor J. D. Jackson. The author would like to thank Professor Jackson for his guidance and generous assistance in the preparation of this paper. The author also wishes to acknowledge useful conversations with Dr. H. Hogaasen, Dr. K. Zalewski, and members of the Track Chamber division at CERN. He is grateful to Professor J. Prentki and Professor L. Van Hove for the hospitality of the Theoretical Studies division at CERN and to the National Science Foundation for a fellowship.

¹⁷ J. S. Lindsey and G. A. Smith, Phys. Rev. **147**, 913 (1966).

¹⁸ S. M. Flatté, Phys. Rev. **155**, 1517 (1967).

¹⁹ W. L. Yen, R. L. Eisner, L. Gutay, P. B. Johnson, P. R. Klein, R. E. Peters, R. J. Sahni, and G. W. Tauffest, Phys. Rev. Letters **18**, 1091 (1967).

²⁰ I. Derado, J. A. Poirier, N. N. Biswas, N. M. Cason, V. P. Kenney, and W. D. Shephard, Phys. Letters **24B**, 112 (1967).

²¹ In particular the exchange contributions of pion and vector-meson trajectories do not interfere in vector-meson production, so our results are not reproduced by such a simple Regge-pole model. However, the exchange of additional trajectories, e.g., A_2 , could produce an interference contributing with opposite signs to K^{*+} and K^{*-} , ω and A_2 having opposite charge-conjugation properties.